P4.21 VALIDATION OF A GLOBAL CLOUD LIQUID WATER PRODUCT FROM AVHRR

Andrew K. Heidinger
NOAA/NESDIS Office of Research and Applications *

Quanhua Liu
Cooperative Institute for Research in the Atmosphere(CIRA)

1. INTRODUCTION

Imagers such as the Advanced Very High Resolution Radiometer (AVHRR) provide high spatial resolution data in spectral regions from the visible to the infrared window. Algorithms have become well-accepted that use a visible reflectance, a near-infrared reflectance and a brightness temperature from a thermal window channel to derive cloud optical depth, cloud particle size and cloud-top temperature. The work of Platnick and Valero(1995) provide a brief history of these algorithms up to 1995.

In this abstract, we present an algorithm which derives the statistical distribution of the cloud optical depth over a large region (a grid-cell) based on the statistical distribution of the visible reflectance and the mean values of other channel observations. This algorithm also estimates the mean cloud particle size and cloud-top temperature. The global validation of this algorithm is ongoing and this abstract serves as an illustration of its methods. One example retrieval is shown to highlight the type of information it provides.

The motivation to develop an algorithm such as this is that the pixel-scale retrievals of cloud properties are computationally expensive. The only pixel-scale processing needed for this algorithm is the application of a cloud mask and the accumulation of the grid-cell reflectance/radiance statistics. The goal of this work is develop an algorithm which can produce global cloud properties in real-time and can be used to efficiently reprocess the AVHRR data-record into new cloud climatologies which reflect ongoing improvements in cloud radiative transfer.

1 Methodology

Inspection of a single-layer cloud field within a grid-cell reveals that the cloud-top particle size and cloud top temperature typically do not vary significantly while the cloud optical depth can vary greatly. To illustrate this point, the results for a single grid-cell are analyzed. Fig. 1 shows the distribution of NOAA16 AVHRR GAC ch1 (0.63 μm) reflectance a stratus cloud field off the coast of California. Fig. 2 shows the ch1 values for one grid-cell that is outlined in Fig. 1. This grid-cell has a spatial resolution of 110 km which is the resolution of the AVHRR Pathfinder Atmospheres (PATMOS) data-set and is the resolution used for the global implementation of this algorithm. Plane parallel retrievals of the optical depth, τ, effective radius, r_e and the cloud-top temperature T_c where performed on each pixel determined to be cloudy. This resulted in over 600 retrievals for this one grid-cell. Fig. 3 shows the distributions of τ, r_e and T_c for this grid-cell. This distributions are normalized to have maximum of unity and the values of T_c are offset by 260 K to allow for plotting on the same axes.

Based on analysis of data as shown in Fig. 3, we make the assumption that a representative description of the cloudiness for a single cloud layer within a grid-cell can be given by the mean values of r_e and T_c and the distribution τ. The algorithm we have developed provides this information on global and real-time basis.

To model the statistical distribution of cloud optical depth in a grid-cell, $p(\tau)$, a modified Γ distribution is assumed and the form used is

$$p(\tau) = \frac{1}{\Gamma(\nu)} \left(\frac{\nu}{\bar{\tau}}\right)^{\nu} \tau^{\nu-1} \exp^{-\frac{\nu\tau}{\bar{\tau}}} \qquad (1)$$

where τ is the optical depth, ν is the width parameter, and $\bar{\tau}$ is the mean optical depth. The standard deviation of τ, σ_τ, is given by $\left(\frac{\bar{\tau}}{\nu}\right)^2$. The justification for the choice of the Γ distribution is given by inspection results similar to Fig. 3 and by the work of Barker et al. (1996) where many high spatial resolution cloud optical depth fields were produced from LandSat data using pixel-level retrievals. Barker et al. (1996) divided the LandSat scenes into three classes (A: Overcast Stratocumulus, B: Broken Stratocumlus, C: Scattered Cumulus). The ranges in $\bar{\tau}$ the for cases A,B and C were 5.6-20.5, 3.4-15.6,

*Corresponding author address: Dr. Andrew K. Heidinger, NOAA/NESDIS Office of Research and Applications, Washington, DC 20746-4304, USA; e-mail: andrew.heidinger@noaa.gov

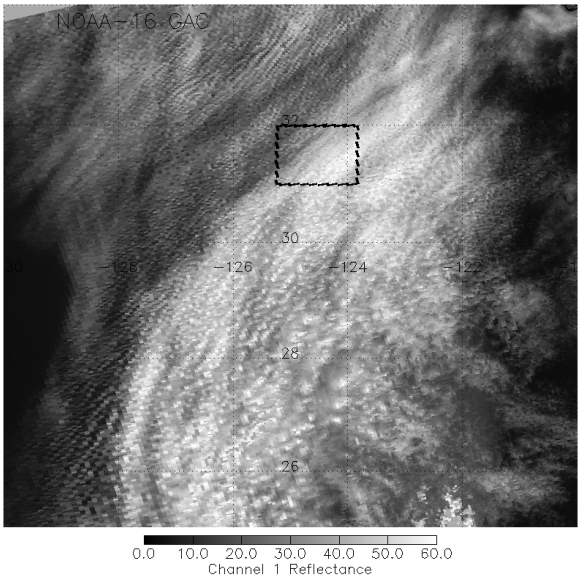

Figure 1: AVHRR Ch1 reflectance from NOAA-16 for a stratus cloud field off the coast of California

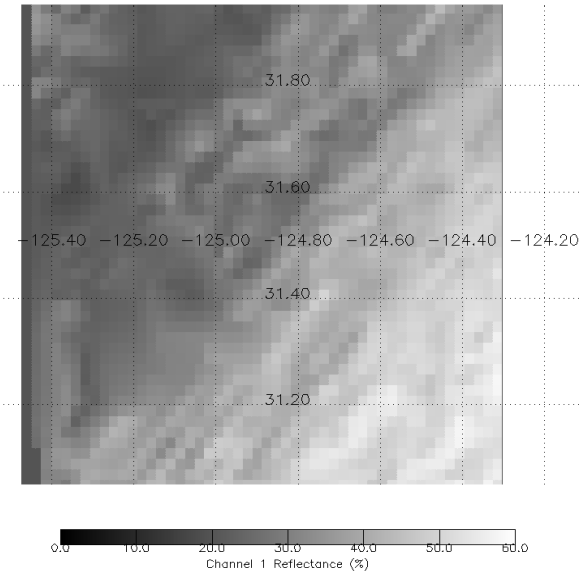

Figure 2: Variation of ch1 reflectance for grid-cell outlined in Fig. 1

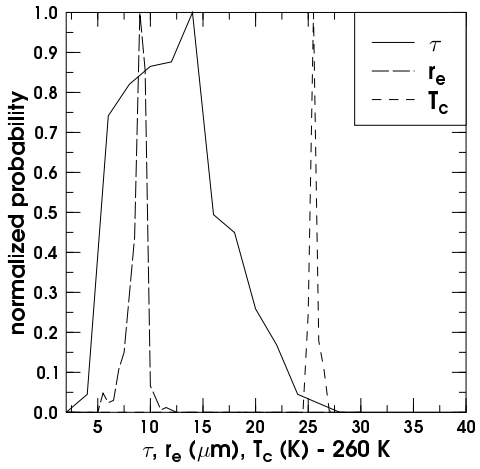

Figure 3: Histograms of pixel-level retrievals for τ, r_e, and T_c for grid-cell outlined in Fig. 1

1.0-12.1. The ranges in ν the for cases A,B and C were 1.6-22.5, 0.74-1.7 and 0.2 - 1.9. A similar study for non-boundary layer clouds has not been undertaken. However as long as the reflectance distributions from cloudy pixels are mono-model, a Γ distribution should adequately model the distribution of τ.

2 Retrieval Methodology

To retrieve the cloud parameters, a one-dimensional variational (1D-var) technique is used. In this retrieval 4 parameters are being estimated from 4 observations. A 1D-var approach was selected since more traditional iterative approaches such as applied by (Han et al. 1994) were found to offer no advantage in speed or in convergence. A 1D-var approach also offers the benefits of ensuring the retrievals are consistent with the forward models and the known uncertainty of the measurements.

The form of the 1D-var retrieval methodology used here is taken from Rodgers (1976). Using Rodger's notation, the vector of measurements, $\tilde{y}$, for this algorithm is given by

$$\tilde{y} = (R_1, R_{3a}, E_4, \sigma_1)$$

where R_1 is the mean channel 1 reflectance, R_{3a} is the mean channel 3a reflectance, E_4 is the mean channel 4 radiance, and σ_1 is the standard deviation of the channel 1 reflectance. The mean and

standard deviations are defined for all cloudy pixels of the same cloud type within a grid-cell.

The vector of estimated parameters, x, is defined as

$$\tilde{x} = (\bar{\tau}, r_e, T_c, \nu)$$

where $\bar{\tau}$ is the mean optical depth, r_e is the effective radius, T_c is the mean cloud-top temperature and ν is the width of $p(\tau)$. In addition, this retrieval method requires the definition of *a priori* estimates of $\tilde{x}$ which are derived based on representative values for each cloud type. The final solution is an optimal estimate of $\tilde{x}$ that reflects the uncertainties in the measurements, the forward models and the *a priori* parameters.

2.1 Forward Modeling

The goal of the forward models put forth here is to simulate the true behavior of cloud fields within grid-cells well enough to allow for meaningful estimation of their properties. Since global, faster than real-time processing is required of this algorithm, true radiative transfer models are approximated by lookup tables. The forward models described here are similar to the forward models used in pixel-scale retrievals except that the width of the τ distribution for a grid-cell, ν, is used. The forward models described below provide the vector, $\tilde{f}$, which contains the forward model estimate of $\tilde{y}$ and the kernel matrix, $\tilde{K}$ where each element contains $\frac{\partial f}{\partial x}$.

2.2 Modeling Solar Reflectance

To model the observed solar reflectance, a lookup table is computed using an adding/doubling model for the reflectance of an plane parallel cloud above a dark surface with no other atmospheric effects, R_c. Once the lookup tables for single layer plane parallel clouds are made, lookup tables with the additional dimensions of ν and surface reflectance, a_s, are made. To compute the top of atmosphere reflectance for a plane parallel cloud above a reflecting surface, the following expression taken from Chandrasekhar (1960) is used.

$$R = t_{ac}^m \left(R_c + \frac{T(\mu) a_s' T(\mu_o)}{1 - a_s' \alpha_{sph}} \right) \qquad (2)$$

where α_{sph} is the spherical albedo of the cloud layer, t_{ac} is the nadir transmission from the top of atmosphere to cloud-top, and m is the airmass factor ($\frac{1}{\mu} + \frac{1}{\mu_o}$). The terms $T(\mu)$ and $T(\mu_o)$ are the flux transmissions through the cloud layer (direct and diffuse) for a solar beam incident at zenith angles defined by μ and μ_o. The modified surface albedo,a_s', accounts for absorption between the cloud and the surface and is approximated as

$$a_s' = t_{bc}^m a_s$$

t_{bc} is the nadir transmission from the cloud to the surface.

The final mean reflectance for a distribution of optical depth, $\bar{R}(\bar{\tau}, \nu)$ is given by integrating (2) over the assumed $p(\tau)$ to give

$$\bar{R}(\bar{\tau}, \nu) = \int_0^\infty R_{pp}(\tau) p(\tau) d\tau \qquad (3)$$

with the standard deviation, σ_R being computed as

$$\sigma_R = \sqrt{\int_0^\infty \left(\bar{R}(\bar{\tau}, \nu) - R_{pp}(\tau) \right)^2 p(\tau) d\tau} \qquad (4)$$

The result of these computations are lookup tables for the mean and the standard deviation in reflectance as a function of the cloud properties, τ, r_e, ν, the surface reflectance, a_s, and the viewing geometry, $\mu, \mu_o, \phi_o - \phi$.

2.3 Modeling Thermal Emission

In a similar manner to modeling of solar reflectance, an adding/doubling model is used to compute the emissivity, ϵ_c and transmissivity, t_c, for an isolated isothermal cloud. The emissivities and transmissivites include the effects of scattering within the cloud layer. Values of the mean emissivity and transmissivity are computed using the plane parallel lookup tables and equation (3).

Once the lookup tables of emissivity and transmissivity are made as functions of $\bar{\tau}, \nu, r_e$ and θ, the cloud layer is embedded in a non-scattering atmosphere to model to the top of atmosphere radiance using the following relation.

$$E = E_{ac}(1 - t_{ac}^m t_c) + t_{ac}^m \left(\epsilon_c B(T_c) + t_c E_{clear} \right) \qquad (5)$$

where E_{clear} is the clear-sky radiance, E_{ac} is the emitted radiance from the layer above the cloud, and m is airmass for emitted radiation ($\frac{1}{\mu}$). To account for the lapse rate within the cloud, the cloud emissivity is redefined. Using a linear-in-depth variation of the emission through the cloud, a modified emissivity of the cloud, ϵ_c' can be computed to account for temperature variations using the following relation.

$$\epsilon_c' = \epsilon_c (1 - \frac{B_n}{B_o} e^{-\tau/\mu} + (1 - e^{-\tau/\mu}) \frac{(B_n - B_o)}{\tau B_o}$$

where B_n and B_o are the black-body emitted radiances at the cloud top and cloud base.

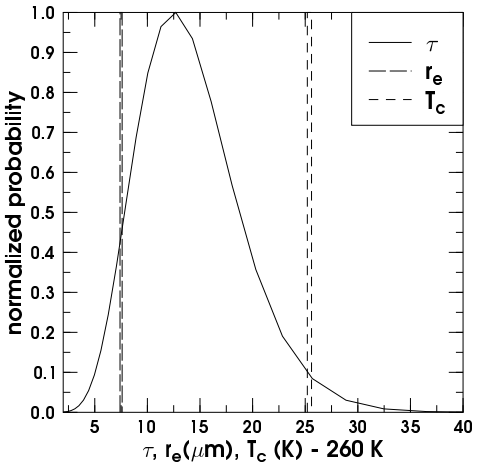

Figure 4: Results of grid-cell retrieval for τ, r_e, and T_c for grid-cell outlined in Fig. 1

3 Results

To illustrate how the retrieval works, the retrieval results for the grid-cell outlined in Fig. 1 are shown. This grid-cell consisted of only one layer of cloud. The pixel-level retrievals shown in Fig. 3 gave the values shown in Table 1. The values from the grid-cell retrieval are also shown in Table 1. The distribution of τ shown in Fig. 3 is computed from the retrieved values of $\bar{\tau}$ and ν.

	pixel	grid-cell
$\bar{\tau}$	13.5	12.6
ν	8.0	7.4
r_e	9.0	7.5
T_c	285.2	285.5

Table 1: Comparison of retrieved cloud properties using the grid-cell retrieval and the pixel-level retrieval for grid-cell outlined in Fig 1.

As the results in Table 1 indicate, differences can exist between the grid-cell and the pixel-level retrieval for some grid-cells. In this example, the mean effective radius from all the pixel-level retrievals in this grid-cell was 1.5 μm larger than the value estimated by the grid-cell retrieval. The differences between the two approaches do not appear to be biased in any one direction. Work is ongoing to understand the reason and physical meaning of the differences between the grid-cell and pixel-level retrievals.

4 Conclusions

A retrieval has been developed to produce real-time cloud products from AVHRR. A preliminary global implementation of this algorthm has already been performed using NOAA-16 AVHRR data. A global validation of these cloud products including the derived cloud liquid water path is being undertaken. This validation includes comparison with cloud properties from microwave sensors. Other areas of research include the optimal combination of the AVHRR products with those from microwave sensors. This work is supported by the NOAA/NASA Joint Center for Data Assimilation.

5 References

Barker, H. B. Wielicki, L. Parker, 1996: A parameterization for computing grid-averaged solar fluxes for inhomogeneous marine boundary layer clouds. Part II: Validation using satellite data. *J.Atmos. Sci.*, **53**, 2304- 2316.

Chandrasekhar, 1960: *Radiative Transfer.* Dover Publications Inc., 393 pp.

Platnick, S and F. P. J. Valero, 1995: A validation of a satellite cloud retrieval during ASTEX. *J. Atmos. Sci.*, **52**, 2985-3001.

Rodgers, C. D., 1996: Retrieval of atmospheric temperature and composition from remote measurements of thermal radiation. *Rev. Geophys. Space. Phys.*, **14**, 609-624.